Inflammatory Conditions Promote Resistance to Immune Checkpoint Inhibitors in High Microsatellite Instability Colorectal Cancer

Qiaoqi Sui
Sun Yat-sen University Cancer Center https://orcid.org/0000-0001-5191-218X
Xi Zhang
Beijing Genomics Institute
Jinghua Tang
Department of Colorectal Surgery, Sun Yat-sen University Cancer Center
Kai Han
Sun Yat-sen University Cancer Center https://orcid.org/0000-0002-8688-8017
Wu Jiang
Sun Yat-sen University Cancer Center
Liao Leen
Sun Yat-sen University Cancer Center
Lingheng Kong
Sun Yat-sen University Cancer Center
Yuan Li
Sun Yat-sen University Cancer Center
Zhenlin Hou
Sun Yat-sen University Cancer Center
Chi Zhou
Sun Yat-sen University Cancer Center
Chenzhi Zhang
Sun Yat-sen University Cancer Center
Linjie Zhang
Sun Yat-sen University Cancer Center
Binyi Xiao
Sun Yat-sen University Cancer Center
Wei-Jian Mei
Sun Yat-sen University Cancer Center https://orcid.org/0000-0002-0025-2908
Yanbo Xu
Sun Yat-sen University Cancer Center
Jian Zheng

Sun Yat-sen University Cancer Center https://orcid.org/0000-0001-9831-7038

Zhi-Zhong Pan

Sun Yat-sen University Cancer Center

Pei-Rong Ding (dingpr@sysucc.org.cn)

Sun Yat-sen University Cancer Center https://orcid.org/0000-0002-0796-8175

Article

Keywords: Inflammatory Conditions, dMMR/MSI-H CRCs, Immune Checkpoint Inhibitors, Neutrophils, CTLA-4

Posted Date: September 27th, 2021

DOI: https://doi.org/10.21203/rs.3.rs-898644/v1

Abstract

Inflammatory conditions are common complications in colorectal cancer (CRC) and play significant roles in tumor progression and immunosuppression. However, the influence of inflammatory conditions on the tumor response to immune checkpoint inhibitors (ICIs) remains unclear. We included a high microsatellite instability (MSI-H) CRC patient whose primary tumor progressed and liver metastasis regressed after Pembrolizumab treatment. An organoid-T cell coculture model demonstrated an inhibited local immune response instead of systemic immunosuppression. Single-cell RNA sequencing suggested that neutrophils suppress the immune microenvironment, mostly through CTLA-4-associated pathways. A cohort of 73 patients with MSI-H CRC who received ICIs were enrolled, among whom inflammatory conditions were correlated with a poor tumor response. We demonstrated that inflammatory conditions in MSI-H CRCs correlate with resistance to ICIs through neutrophil-associated immunosuppression. Additional CTLA-4 blockade may improve the sensitivity to PD-1 blockade. Clinically, inflammatory conditions could predict a poor response to ICIs in MSI-H CRCs.

Introduction

High microsatellite instability (MSI-H), highly correlated with DNA mismatch repair deficiency (dMMR), plays a prominent role in the tumorigenesis of colorectal cancer (CRC)[1,2]. dMMR and MSI-H are associated with high mutation burden, high tumor neoantigen load and dense infiltration of immune cells[3,4]. It has been well accepted that a dMMR/MSI-H status benefits CRC patients receiving immune checkpoint inhibitors (ICIs), especially PD-1 blockade[5,6]. However, recent studies have reported that the immune status differs among dMMR/MSI-H CRCs, and over 50% of patients still experience resistance to ICIs with an unclarified mechanism[6].

It has been revealed that both local and systemic inflammation have important roles in tumorigenesis, disease progression, and patient prognosis in various cancers[7–9]. Recently, studies found that inflammation is also associated with immunosuppression, and elevated inflammatory cells in the tumor microenvironment are associated with resistance to ICIs[10–12]. In addition, the inflammatory response is associated with alterations in peripheral blood leukocytes that can be captured by a high neutrophil-to-lymphocyte ratio (NLR), which is also associated with poor long-term survival across all ICIs in patients with various soild tumors[13–15].

Inflammatory conditions caused by obstruction or perforation are common complications in CRCs, while their significance in the response to ICIs remains unclarified in MSI-H CRCs. Here, we investigated the impact of inflammatory conditions on dMMR/MSI-H CRC patients receiving ICIs.

Results

Inflammatory conditions are associated with resistance to ICIs in dMMR/MSI-H CRCs

A 35-year-old woman with metastatic MSI-H descending colon cancer, who had peritonitis due to perforation of primary tumor and received transverse colostomy, was enrolled (Patient 1). The primary tumor and liver metastatic lesions regressed after 3 courses of Pembrolizumab in the combination of chemotherapy. After 5 courses of treatment, the patient had a fever, with increased white blood cell count and C-reactive protein concentration. She was considered having immune-related adverse reactions, and received only chemotherapy at the sixth course. After 6 courses of treatment, the primary tumor was diagnosed progressing with elevated tumor markers, and recurrent fever remained. The patient was then considered having localized infection in the perforating site and received another 3 courses of Pembrolizumab treatment combined with anti-infective therapy (Supplementary Fig. 1). The primary tumor continued to progress. Meanwhile, the metastatic lesions continually regressed after 9 courses of treatment (Fig. 1A). The patient finally received resection of primary tumor and 15 courses of postoperative Pembrolizumab. The liver metastases were evaluated as complete remission and remained no evidence of diseases on last follow-up in July 2021.

Patient 1 achieved mixed response in primary tumor (progressive disease, PD) and metastatic tumor (partial response, PR) after 5 courses of Pembrolizumab combined with chemotherapy and one course of chemotherapy. Localized infection around the primary tumor was noticed and considered to be one of the potential reasons leading to the resistance of primary tumor. We therefore hypothesized that local inflammatory conditions could be associated with resistance to ICIs. To demonstrate this, a cohort of 73 dMMR/MSI-H CRC patients who received ICIs was retrospectively included (Table 1). We found that inflammatory conditions during ICI treatment were correlated with a higher ratio of stable disease (SD) and PD (87.5% vs. 33.3%, $P < 0.001$) and worse progression-free survival (PFS) ($P = 0.001$) (Fig. 1B and C). Multivariate Cox proportional hazards regression indicated that inflammatory conditions were independently associated with the risk of progression (Table 2).

Table 1
Baseline characteristics of 73 MSI-H CRC patients receiving ICIs

	With inflammatory conditions	Without inflammatory conditions	*P* value
Total	16	57	
Gender			0.533
Male	10 (62.5%)	42 (73.7%)	
Female	6 (37.5%)	15 (26.3%)	
Median age (range)	42 (16–73)	42 (24–71)	0.714
MSI status			0.417
MSI-H	11 (68.8%)	40 (70.2%)	
MSI-L/MSS	4 (25.0%)	8 (14.0%)	
Undetermined dMMR	1 (6.2%)	9 (15.8%)	
Category			0.367
Sporadic	3 (18.8%)	17 (29.8%)	
Lynch-associated	7 (43.7%)	28 (49.1%)	
undetermined	6 (37.5%)	12 (21.1%)	
Histology			0.231
Adenocarcinoma	11 (68.8%)	47 (82.5%)	
Mucinous Adenocarcinoma	5 (31.2%)	10 (17.5%)	
ICI monotherapy			0.704
Yes	7 (43.7%)	28 (49.1%)	
No	9 (56.3%)	29 (50.9%)	
First-line chemotherapy prior to ICIs			0.028
Yes	4 (25.0%)	32 (56.1%)	
No	12 (75.0%)	25 (43.9%)	

Table 2
Univariate and multivariate Cox proportional hazards regression for PFS.

Variable	No. of cases	*HR* (95% *CI*)	*P*
MSI status			
MSI-H	52	1.000 (ref)	——
MSI-L/MSS	11	3.536 (1.281 ~ 9.759)	0.015
Inflammatory conditions			
No	57	1.000 (ref)	——
Yes	16	5.393 (2.121 ~ 13.712)	< 0.001
Histology			
Adenocarcinoma	58	1.000 (ref)	——
Mucous adenocarcinoma	15	2.239 (0.867 ~ 5.781)	0.096
Multivariable			
MSI status			
MSI-H		1.000 (ref)	——
MSI-L/MSS		2.497 (0.806 ~ 7.730)	0.113
Inflammatory conditions			
No		1.000 (ref)	——
Yes		3.637 (1.255 ~ 10.538)	**0.017**
Histology			
Adenocarcinoma		1.000 (ref)	——
Mucous adenocarcinoma		1.112 (0.353 ~ 3.502)	0.856

We then constructed tumor organoids of Patient 1, Patient 2 and Patient 3, among whom only Patient 1 had inflammatory conditions (Fig. 1D). Patients 1 and 2 had PD and SD, while Patient 3 was diagnosed with complete response (CR) after ICIs. Tumor organoids were cocultured with paired TILs or T cells from peripheral blood mononuclear cells (PBMCs). We observed that the apoptotic proportion of organoid cells was higher in the PBMC group in Patient 1 and was higher in the TIL group in Patient 3, while the proportions in Patient 2 were comparable between those two groups. In addition, Patient 1 and Patient 3 had comparable apoptotic proportions in the PBMC coculture group, yet the apoptotic proportion in the TIL group was the lowest in Patient 1 (Fig. 1E). These phenomena indicate an inhibited local immune response to tumors instead of systemic immunosuppression in Patient 1.

An inhibitory role of neutrophils in the tumor immune status is revealed by single-cell RNA sequencing (scRNA-seq)

To investigate the component of the microenvironment in the primary tumor of Patient 1, scRNA-seq was conducted. The 4489 qualified cells were divided into epithelial cells and immune cells (Fig. 2A and B). The CNV landscape analysis showed that most of the epithelial cells (Epithelial-1 to Epithelial-6, Epithelial-8) were malignant tumor cells, which were characterized by frequent copy number loss and deletion in several chromosomes (Supplementary Fig. 2 and Supplementary Table). Among immune cells, CD8 + T cells were mainly identified as exhausted cells expressing *PDCD1* and *KLRD1* separately (CD8 TEX PDCD1 and CD8 TEX KLRD1). In addition, CD4 + T cells were mainly regulatory T cells (Treg cells) expressing *FOXP3* (with or without *CTLA-4* expression). In addition, 132 myeloid cells were identified, which were characterized by high expression of *PTPRC, C1QB, AIF*, and *LYZ* (Supplementary Fig. 3 and Supplementary Table). Furthermore, myeloid cells expressed *FCGR2A, FCGR3A, FCGR3B, CD44* and *CD55*, which indicated that they are neutrophil-like cells (Fig. 2C)[16–18].

To further investigate the interaction between immune cells, a cell-cell network analysis was conducted, suggesting that myeloid cells had a core role in the immune microenvironment, as they harbored the most connections with other cell types, especially with exhausted CD8 + T cells (Fig. 2D). To further investigate the interactions that occur in the ecosystem, a significant L-R pair was conducted to calculate the intensity of the interactions, which suggested crosstalk between myeloid cells and T cells via CTLA-4-CD80/CD86 (Fig. 2E). Other L-R pairs involving chemokines and cytokines between myeloid cells and T cells were also identified, including CCL5-CCR1, CCL5-CCR5, CCL3-CCR5, TNF-TNFRSF1B, IFNG-type II IFNR, and CSF1R-CSF1 (Supplementary Fig. 4).

To investigate the role of the CTLA-4-CD80/CD86 axis in the exhaustion of T cells under inflammatory conditions, PD-1 neutralized murine T cells were stimulated in the presence or absence of neutrophils before coculture with CT26 cells. The apoptosis assays suggested that additional treatment with CTLA-4 neutralizing antibody for T cells augmented the apoptotic proportion of CT26 cells. More importantly, coculturing with neutrophils attenuated the cytotoxicity of T cells, while this effect could be rescued by CTLA-4 neutralization (Fig. 2F).

Elevated neutrophil infiltration is associated with a poor immune status and poor response to ICIs.

To investigate the influence of neutrophils on MSI CRCs, The Cancer Genome Atlas (TCGA) data were analyzed using ImmunCellAI. We found that poor response to ICIs was associated with elevated neutrophil infiltration (Fig. 3A). Moreover, neutrophil infiltration negatively correlated with total infiltration scores (Fig. 3B) and the infiltration of cytotoxic T cells, Th1 cells, NK cells and B cells (Fig. 3C). To validate our findings, data were further analyzed using The Cancer Immunome Atlas (TCIA) and Tumor Immune Estimation Resource (TIMER). We still found that elevated neutrophils were associated with lower immunophenoscores (IPS) and poor overall survival (OS) in MSI CRCs.

An elevated NLR is associated with a poor immune status and resistance to ICIs in dMMR/MSI-H CRC

According to a previous study, the NLR shows a positive correlation with infiltrating neutrophils in tumors[19]. In a cohort of 142 surgically resected dMMR/MSI-H CRCs, we demonstrated that the CD8 + TILs in the IM and CN were significantly lower in patients with an NLR > 3 (Fig. 4A). To demonstrate that the NLR could predict the tumor response to ICIs, clinical data from the 73 samples were analyzed. We found that patients with inflammatory conditions had higher NLRs (Fig. 4B) and that patients with an NLR > 3 had a higher SD + PD ratio (57.6% vs. 35.0%, $P = 0.025$) and worse PFS ($P = 0.022$) after receiving ICIs (Fig. 4C and D). To compare the efficiency between the NLR and inflammatory disease in predicting tumor response to ICIs, ROC curves were used. The AUC of having an inflammatory condition was 0.723 ($P = 0.005$, 95% *CI*, 0.572 ~ 0.874), while the AUC of an NLR > 3 was 0.642 ($P = 0.071$, 95% *CI*, 0.495 ~ 0.790). When two predictors were combined, the AUC was 0.758 ($P = 0.001$, 95% *CI*, 0.618 ~ 0.897) (Supplementary Fig. 5).

Discussion

ICIs are very effective treatments for patients diagnosed with MSI-H CRCs, but 30–50% of patients present primary or secondary resistance to the treatment[5,20]. In the present study, we demonstrated that MSI-H CRC patients with inflammatory conditions have higher risks of resistance to ICIs through neutrophil-associated T cell exhaustion. In addition, both inflammatory conditions and a high NLR predict a poor response to ICIs, and the prognostic value was further increased when these two predictors were combined.

Prior to the current study, the influence of neutrophils on immune status and ICI response has been revealed[21]. Tumor-associated neutrophils are generally considered to promote tumorigenesis among multiple tumor types, and there are also studies regarding neutrophils establishing a pre-metastatic niche for tumor cells[22–25]. In pancreatic cancer, it has been found that IL17-induced neutrophil extracellular traps could mediate resistance to ICIs[10], and neutrophils in tumors effectively suppress normal T-cell immunity in gastric cancer[26]. In the current study, we have significantly expanded upon these previous observations. The current study demonstrates that both local inflammatory conditions and the NLR are associated with a poor immune status and a poor tumor response to ICIs, and the cell-cell network analysis in Patient 1 indicated that neutrophils play a prominent role in immunosuppression in MSI-H CRCs.

Although neutrophils can be activated by inflammatory conditions, our findings indicate that neutrophils in tumors are functionally distinct from their peripheral counterparts, since different cytotoxicities between T cells in peripheral blood and TILs were observed. Apart from our study, Wang et al also revealed that tumor-infiltrating neutrophils exhibited an activated phenotype compared with normal activated peripheral cohorts[26]. In addition, multiple cell types in the tumor microenvironment could contribute to the pool of cytokines including G-CSF, GM-CSF, CXCR2 ligands and IL17, which activate neutrophils and educate other immune cells to be tumor-associated[26,27]. Therefore, tumor-infiltrating neutrophils are thought to contribute more to immunosuppression than peripheral neutrophils.

Studies have suggested that the induction of PD-L1 by inflammatory factors may be one of the most important factors affecting the therapeutic efficiency of PD-1 blockade[12,26]. However, the current study indicated that the CTLA-4-CD80/CD86 axis also participate in the interaction of neutrophils and T cells. More significantly, an in vitro experiment demonstrated that CTLA-4 neutralization may reduce the inhibitory function of neutrophils on T cells. Depleting immunosuppressive tumor-associated myeloid cells is an attractive therapeutic approach to promote antitumor immune responses[28,29]. However, these inhibitors have provided minimal therapeutic benefits in cancer patients as monotherapies, and whether these treatments could restore sensitivity to ICIs remains unclear. Because ICIs directed against PD-1 and CTLA-4 are highly effective in dMMR/MSI-H CRCs, and CTLA-4 blockade reduces immature myeloid cells in cancers[30], blockade of the CTLA-4 axis may be appropriate for MSI-H CRC patients with inflammatory conditions.

CD80/CD86 appears to play a central role in inflammatory diseases[31,32]. As a response to hypoxia and specific cytokines, myeloid cells express elevated levels of CTLA-4 ligands and other immune checkpoint inhibitors. CTLA-4 ligands such as B7 molecules are also highly expressed in dendritic cells[33]. In T cells, CTLA-4 and CD28 exist as homodimers capable of binding to CD80/CD86 via the same extracellular motif. Some researchers have claimed that upregulating CD80 in neutrophils could promote the activation of T cells by interacting with CD28[34], while others have suggested that CTLA-4 has a substantially higher affinity and avidity, thereby outcompeting CD28 and simply preventing it from eliciting its stimulatory signals[30,35]. Together, these findings suggest that the interaction of CTLA-4 and CD80/CD86 contributes most to T cell exhaustion under inflammatory conditions.

It has also been shown that elevated neutrophils in peripheral blood predict poor prognosis and resistance to ICIs in multiple cancers[36,37]. In the study of Fan et al., an NLR > 5 was associated with poor clinical response to anti-PD-1 therapy in patients with advanced gastric and colorectal cancers[38]. In metastatic MSI-H CRC, the pan-immune-inflammation value, calculated using routine blood test data, is a strong predictor of outcome in patients receiving ICIs [39]. In the current study, an NLR > 3 was also identified as a predictor of poor ICI response. The detection of neutrophil frequency, NLR, or neutrophil-releasing factors in patients' serum is easy, inexpensive, and applicable. Additionally, in cancer patients without inflammatory conditions, an elevated NLR is associated with worse immune status and poor ICI response[40]. Since the AUC of the inflammatory condition combined with the NLR was larger than that of single factors, we consider that in MSI-H CRCs, patients with inflammatory conditions could have a poor tumor response to ICIs. Among patients without inflammatory conditions, an NLR > 3 could be a promising predictor for a poor response to ICIs.

In conclusion, the current study demonstrates that inflammatory conditions in MSI-H CRCs correlate with resistance to ICIs through neutrophil-associated immunosuppression, and additional CTLA-4 blockade may potentially improve the sensitivity among those patients. Clinically, both inflammatory conditions and an NLR > 3 could predict a poor tumor response to ICIs in MSI-H CRCs.

Methods

Patient inclusion and follow-up

Patients with MSI-H CRC from Sun Yat-sen University Cancer Center (SYSUCC, Guangzhou, China) who received ICI treatment were enrolled. The exclusion criteria were as follows: 1) receiving only postoperative ICIs after radical surgery; 2) receiving less than 2 courses of ICIs. Finally, 73 patients were enrolled. In addition, dMMR/MSI-H CRC patients who received surgical treatment with sufficient tumors for counting tumor-infiltrating lymphocytes (TILs) were enrolled as previously described[41]. Follow-up data, blood test, CT scanning, and determination of responses to ICIs were collected from the tracking system. Tumor responses were determined as complete response (CR), partial response (PR), stable disease (SD) and progressive disease (PD). Patients who had obstructions, perforations, peritonitis, or other radiologically diagnosed inflammation in abdominal viscera caused by tumors were considered to have inflammatory conditions.

Organoids

Tumor tissues of three MSI-H CRCs (Patient 1, Patient 2 and Patient 3) were collected. Tissue from Patient 1 was collected after 9 courses of Pembrolizumab, and tissues from Patients 2 and 3 were collected prior to ICIs. Tumors were digested with digestion buffer (RPMI 1640 medium (Gibco) containing 10% fetal bovine serum (FBS), 1% penicillin-streptomycin, 4 mg/mL collagenase [Sigma C5138]) and embedded in Matrigel (Corning). After solidification, the Matrigel was overlaid with IntestiCult OGM Human (Stem Cell) supplemented with penicillin (100 U/mL), streptomycin (100 μg/mL) and 10 mM Y-27632 (Sigma-Aldrich) at 37°C with 5% CO_2. Organoids used in experiments were under passage 10. Hematoxylin and eosin (HE)-stained sections of organoids were assessed by pathologists to determine the tumor status. For HE staining, Matrigel samples were fixed with formalin at 4°C overnight and coated with a 5% agarose gel before paraffin imbedding.

Preparation and treatment of human T cells

Paired peripheral blood mononuclear cell (PBMC)-derived T cells and TILs from 3 MSI-H CRC patients (Patient 1, Patient 2 and Patient 3) were isolated using a human pan-T cell isolation kit according to the manufacturer's instructions (Miltenyi Biotec). Human T cells were cultured in Human ImmunoCult-XF T Cell Expansion medium (Stem Cell) with penicillin (100 U/ml) and streptomycin (100 μg/ml) at 37°C with 5% CO_2. Cells were prestimulated with IL-2 (200 U/ml, Peprotech), anti-CD3 (Peprotech) and anti-CD28 (Peprotech) for 48 hours in the presence of paired CRC organoid cells.

Organoid-T cell coculture

To evaluate the cytotoxicity of T cells, organoids were dissociated into single cells and plated (5×10^4 per well) in a 24-well plate in the absence of Matrigel 24 hours before coculture. Pretreated T cells (1×10^6) were added to each plate. After 6 hours, tumor cells were obtained. Using an Annexin V Apoptosis

Detection Kit (Dojindo), the cells were resuspended in phosphate buffered saline (PBS) for cell apoptosis analysis using a Beckman CytoFLEX FCM (Beckman Coulter). The proportion of apoptosis was calculated using FlowJo V10 (BD). Each experiment contained 3 replicates and was repeated three times.

Preparation and treatment of murine neutrophils and lymphocytes

Neutrophils from female BALB/c mice (8 weeks old) were derived from the bone marrow using the mouse Neutrophil Isolation Kit (Miltenyi Biotec), and were cultured in RPMI 1640 supplemented with 10% FBS, penicillin (100 U/ml), and streptomycin (100 μg/ml) at 37°C with 5% CO2. Neutrophils were stimulated with mouse recombinant GM-CSF (Peprotech) for 24 hours in the presence of CT26 cells.

T cells for CT26-T cell coculture were isolated from the spleens BALB/c mice with mouse pan-T cell isolation kits (Miltenyi Biotec) according to the manufacturer's instructions. T cells were cultured in RPMI 1640 supplemented with 10% FBS, penicillin (100 U/ml), and streptomycin (100 μg/ml) at 37°C with 5% CO2. Before experiments, T cells were prestimulated with mouse IL-2 (200 U/ml, Peprotech), anti-CD3 (Peprotech) and anti-CD28 (Peprotech) in the presence of CT26 cells for 48 hours. T cells were also treated with 1 μg/ml anti-PD-1 neutralizing antibody (BioXcell) in the presence or absence of anti-CTLA-4 neutralizing antibody (BioXcell) for 24 hours. For neutrophil-T cell coculture, T cells were cocultured with prestimulated neutrophils at a 2:1 ratio in RPMI-1640 medium for another 24 hours.

CT26-T cell coculture

CT26 cells were plated in a 24-well plate and left overnight in the presence of 200 ng/ml mouse IFN-γ (Peprotech). T cells were added to the tumor cells at a 20:1 ratio at 37°C and cocultured for 12 hours. Using an Annexin V Apoptosis Detection Kit, the CT26 cells were resuspended in PBS for cell apoptosis analysis using a Beckman CytoFLEX FCM. The proportion of apoptosis was calculated using FlowJo V10. Each experiment contained 3 replicates and was repeated three times.

Single-cell RNA-sequencing (scRNA-seq)

The scRNA-seq was conducted using the primary tumor of Patient 1. An scRNA-seq library was prepared using the DNBelab C4 system as previously described[42]. Briefly, the single-cell suspension was transformed into the scRNA-seq library of barcodes through the steps of droplet encapsulation, emulsification and fragmentation, mRNA capture bead collection, reverse transcription, cDNA amplification and purification. An indexed sequencing library was constructed according to the manufacturer's instructions. The sequencing library was quantified using the Qubit SSDNA Assay Kit (Thermo). DIPSEQ T1 was used for sequencing libraries at the National Gene Bank (CNGB, BGI-SHENZHEN, Shenzhen, China). The read structure was paired with Read 1 and Read 2. Read 1 contained 30 bases, including 10 base pair (bp) cell barcode 1, 10 bp cell barcode 2 and 10 bp unique molecular identifier (UMI), and Read 2 contained 100 transcriptional base sequences and a 10 bp sample index. The FASTQ raw data were converted to a Cell Ranger-specific FASTQ file using an in-house Perl script. These FASTQ files were then processed separately using a modified version of the Cell Ranger count pipeline,

which aligned cDNA reads with the GRCH38 human reference using STAR software (v2.5.3)[43]. The mapped reads were then filtered out for valid cell barcodes and UMIs to generate a gene-cell matrix for downstream analysis.

Unsupervised clustering and cell type annotation

Cell clustering was conducted by the Seurat (v3.1)[44] package in RStudio. Genes expressed in less than 3 cells were filtered out, and cells with fewer than 500 or more than 10,000 genes were excluded. The 3 libraries were then integrated using the "Merge" functions, and the batch effects were checked if the cells were separately distributed with the “DimPlot” function. Then, the integrated data are scaled to calculate the principal component analysis. The first 30 PCs were used to construct the SNN network, and the graph-based clustering method Louvain algorithm was used to identify the cell clusters with a resolution of 0.6. Finally, UMAP is used to visualize the clustering results in two-dimensional space. To annotate each cluster as a specific cell type, we selected some classic markers of immune cells and epithelial cells. The cell types were annotated using a violin diagram. The CNV of each epithelial cell was estimated by the inferCNV package[45], using immune cells as a normal control. The epithelial cell clusters with abnormal CNV patterns were annotated as malignant tumor cells.

Cell-cell interaction analysis

To analyze cell-to-cell interactions, we used CellPhoneDB[46] to identify significant ligand-receptor pairs in samples from Patient 1. For immune cells, ligand-receptor (L-R)-specific interactions between cell types were determined based on the specific expression of the receptors of one cell type and the ligands of another cell type. The interaction score refers to the total average of the average expression value of each ligand-receptor pair in the corresponding cell type interaction pair. The expression amount of any complex exported by CellPhoneDB[46] was calculated as the sum of the expression of the constituent genes.

Analysis of online data

Data on MSI status in The Cancer Immunome Atlas (TCIA), Tumor Immune Estimation Resource (TIMER) and Immune Cell Abundance Identifier (ImmuCellAI) were obtained from The Cancer Genome Atlas (TCGA). The predicted ICI response, infiltration levels of neutrophils, cytotoxic cells, T helper 1 (Th1) cells, natural killer (NK) cells and B cells of MSI CRC cases were also obtained from ImmuCellAI (http://bioinfo.life.hust.edu.cn/ImmuCellAI/#!/). The immunophenoscores (IPSs) of MSI CRC cases were obtained from TCIA (https://tcia.at/home), and the infiltration levels of neutrophils were obtained from TIMER (https://cistrome.shinyapps.io/timer/). The optimal cutoff value for high and low neutrophil infiltration levels in TIMER was determined based on the receiver operating characteristic (ROC) curve of overall survival (OS) in the TCGA.

Immunohistochemistry (IHC) analysis and lymphocyte counting

IHC staining was conducted as previously described[41]. All specimens were prepared as 4 μm FFPE sections. The sections were deparaffinized via a series of decreasing concentrations of ethanol, deionized with H_2O, and rinsed in PBS. Endogenous peroxidase activity was blocked via incubation in 3% H_2O_2 solution in methanol. The antigenic epitopes were unmasked in a decloaking chamber using citrate buffer (10 mM sodium citrate and 0.05% Tween 20, pH 6). The sections were then washed in deionized water, rinsed in PBS, blocked for 30 minutes at room temperature with 5% bovine serum albumin in PBS, and incubated with primary antibodies in a humidified chamber at 4°C overnight. After washing, the sections were incubated with anti-rabbit/mouse IgG monoclonal antibody (DAKO Real Envision) at room temperature for 1 hour. Staining was performed using DAB (DAKO Real Envision), followed by counterstaining using hematoxylin. The areas of the invasive margin (IM), tumor stroma (TS) and cancer nest (CN) were defined. IM was defined as discrete lymphoid reactions in the invasive margin of the tumor. TS was defined as a lymphocytic reaction in the tumor stroma within the tumor mass. CN was defined as lymphocytes in the cancer nests. The number of lymphocytes in high-power fields (HPFs; 400×, 0.028 mm^2, Olympus BX41, Tokyo, Japan) was counted by a pathologist according to the following method: select five HPFs in the IM, TS, and CN; count the positive cells; and take the average.

Statistical analysis

SPSS 19.0 (Chicago, IL) and GraphPad Prism 6 (San Diego, CA) were used for data analysis. Data for continuous and discrete variables are reported as the mean and median respectively. Data for categorized variables are reported as percentages. Student's *t* test was used for the comparison of two sets of quantitative data that deviated from the Gaussian distribution. The Mann-Whitney *U* rank-sum test was used for the comparison of two sets of quantitative data that did not deviate from the Gaussian distribution. The Wilcoxon test was used for the comparison of paired quantitative data that did not deviate from the Gaussian distribution. For Student's *t* test, the mean value is shown, and the standard deviation (*SD*) is displayed by the error bar (mean±*SD*). For the Mann-Whitney *U* rank-sum test, the median value is shown, and the range is displayed by the error bar. The Wald chi-square test was used to compare the differences in categorical parameters.Distributions of progression-free survival (PFS) and OS were determined using Kaplan-Meier methods. Univariate and multivariable Cox proportional hazards models were used to predict the outcomes of influential factors. The Pearson or Spearman rank correlation test was used to measure the relationship between two variables. All *P* values were two-sided, and those <0.05 were considered statistically significant. ROC curves were constructed to quantify the diagnostic performance of the prognostic factors for ICI response by assessing the respective areas under the curve (AUCs) with the 95% confidence intervals (*CIs*).

Declarations

Acknowledgement: We thank Dr. Jianhui Yue and Dr. Chao Chen from BGI-SHENZHEN for their assistance with data analysis. We thank the staff at American Journal Experts (North Carolina, USA) for their assistance with English writing.

Author Contribution: Conceptualisation: QS, XZ and PRD. Methodology: QS, XZ, KH, WJ, LL, LK, YL, ZH, CZ, CZ, LZ, BX, WM, and YX. Data curation: XZ, KH, WJ, LL, BX, JZ and ZP. Writing—original draft preparation: QS and XZ. Writing—review and editing: JT, KH and PRD. Supervision: XZ, ZP and PRD. Project administration: XZ, ZP and PRD. Funding acquisition: JT and PRD. QS, XZ, JT and KH, are joint first authors.

Competing Interests: The authors declare that they have no conflict of interest.

Funding: This study was funded by the National Natural Science Foundation of China (grant numbers 82102873, 82073159 and 81871971).

Data Availability Statement: The data underlying this article are available in the Research Data Deposit at https://www.researchdata.org.cn/ and can be accessed with RDD number RDDB2021001664. Data of scRNA-seq was deposited at the GEO Data Set (GSE179784).

Ethics Committee Approval and Patient Consent: All procedures performed in studies involving human participants were approved by the ethical standards of the Ethics Committee of Sun Yat-sen University Cancer Center (GZR2020-273) and were in accordance with the 1964 Helsinki declaration and its later amendments or comparable ethical standards. Informed consent was obtained from all individual participants included in the study.

References

1 Boland, C. R. *et al.* A National Cancer Institute Workshop on Microsatellite Instability for cancer detection and familial predisposition: development of international criteria for the determination of microsatellite instability in colorectal cancer. *Cancer research* **58**, 5248-5257 (1998).

2 Lynch, H. T. *et al.* Review of the Lynch syndrome: history, molecular genetics, screening, differential diagnosis, and medicolegal ramifications. *Clinical genetics* **76**, 1-18, doi:10.1111/j.1399-0004.2009.01230.x (2009).

3 Dolcetti, R. *et al.* High prevalence of activated intraepithelial cytotoxic T lymphocytes and increased neoplastic cell apoptosis in colorectal carcinomas with microsatellite instability. *The American journal of pathology* **154**, 1805-1813, doi:10.1016/S0002-9440(10)65436-3 (1999).

4 Germano, G. *et al.* Inactivation of DNA repair triggers neoantigen generation and impairs tumour growth. *Nature* **552**, 116-120, doi:10.1038/nature24673 (2017).

5 Le, D. T. *et al.* Mismatch repair deficiency predicts response of solid tumors to PD-1 blockade. *Science* **357**, 409-413, doi:10.1126/science.aan6733 (2017).

6 Le, D. T. *et al.* PD-1 Blockade in Tumors with Mismatch-Repair Deficiency. *The New England journal of medicine* **372**, 2509-2520, doi:10.1056/NEJMoa1500596 (2015).

7 Quail, D. F. & Joyce, J. A. Microenvironmental regulation of tumor progression and metastasis. *Nature medicine* **19**, 1423-1437, doi:10.1038/nm.3394 (2013).

8 Diakos, C. I., Charles, K. A., McMillan, D. C. & Clarke, S. J. Cancer-related inflammation and treatment effectiveness. *The Lancet. Oncology* **15**, e493-503, doi:10.1016/S1470-2045(14)70263-3 (2014).

9 Templeton, A. J. *et al.* Prognostic role of neutrophil-to-lymphocyte ratio in solid tumors: a systematic review and meta-analysis. *Journal of the National Cancer Institute* **106**, dju124, doi:10.1093/jnci/dju124 (2014).

10 Zhang, Y. *et al.* Interleukin-17-induced neutrophil extracellular traps mediate resistance to checkpoint blockade in pancreatic cancer. *The Journal of experimental medicine* **217**, doi:10.1084/jem.20190354 (2020).

11 Binnewies, M. *et al.* Understanding the tumor immune microenvironment (TIME) for effective therapy. *Nature medicine* **24**, 541-550, doi:10.1038/s41591-018-0014-x (2018).

12 Jiang, X. *et al.* Role of the tumor microenvironment in PD-L1/PD-1-mediated tumor immune escape. *Molecular cancer* **18**, 10, doi:10.1186/s12943-018-0928-4 (2019).

13 Guthrie, G. J. *et al.* The systemic inflammation-based neutrophil-lymphocyte ratio: experience in patients with cancer. *Critical reviews in oncology/hematology* **88**, 218-230, doi:10.1016/j.critrevonc.2013.03.010 (2013).

14 Ameratunga, M. *et al.* Neutrophil-lymphocyte ratio kinetics in patients with advanced solid tumours on phase I trials of PD-1/PD-L1 inhibitors. *European journal of cancer* **89**, 56-63, doi:10.1016/j.ejca.2017.11.012 (2018).

15 Sacdalan, D. B., Lucero, J. A. & Sacdalan, D. L. Prognostic utility of baseline neutrophil-to-lymphocyte ratio in patients receiving immune checkpoint inhibitors: a review and meta-analysis. *OncoTargets and therapy* **11**, 955-965, doi:10.2147/OTT.S153290 (2018).

16 Bredius, R. G. *et al.* Role of neutrophil Fc gamma RIIa (CD32) and Fc gamma RIIIb (CD16) polymorphic forms in phagocytosis of human IgG1- and IgG3-opsonized bacteria and erythrocytes. *Immunology* **83**, 624-630 (1994).

17 Berger, M. & Medof, M. E. Increased expression of complement decay-accelerating factor during activation of human neutrophils. *The Journal of clinical investigation* **79**, 214-220, doi:10.1172/JCI112786 (1987).

18 McDonald, B. *et al.* Interaction of CD44 and hyaluronan is the dominant mechanism for neutrophil sequestration in inflamed liver sinusoids. *The Journal of experimental medicine* **205**, 915-927, doi:10.1084/jem.20071765 (2008).

19 He, W. Z. *et al.* Systemic neutrophil lymphocyte ratio and mismatch repair status in colorectal cancer patients: correlation and prognostic value. *Journal of Cancer* **9**, 3093-3100, doi:10.7150/jca.26669 (2018).

20 Overman, M. J. *et al.* Nivolumab in patients with metastatic DNA mismatch repair-deficient or microsatellite instability-high colorectal cancer (CheckMate 142): an open-label, multicentre, phase 2 study. *The Lancet. Oncology* **18**, 1182-1191, doi:10.1016/S1470-2045(17)30422-9 (2017).

21 Akbay, E. A. *et al.* Interleukin-17A Promotes Lung Tumor Progression through Neutrophil Attraction to Tumor Sites and Mediating Resistance to PD-1 Blockade. *Journal of thoracic oncology : official publication of the International Association for the Study of Lung Cancer* **12**, 1268-1279, doi:10.1016/j.jtho.2017.04.017 (2017).

22 Faget, J. *et al.* Neutrophils and Snail Orchestrate the Establishment of a Pro-tumor Microenvironment in Lung Cancer. *Cell reports* **21**, 3190-3204, doi:10.1016/j.celrep.2017.11.052 (2017).

23 Furumaya, C., Martinez-Sanz, P., Bouti, P., Kuijpers, T. W. & Matlung, H. L. Plasticity in Pro- and Anti-tumor Activity of Neutrophils: Shifting the Balance. *Frontiers in immunology* **11**, 2100, doi:10.3389/fimmu.2020.02100 (2020).

24 Wculek, S. K. & Malanchi, I. Neutrophils support lung colonization of metastasis-initiating breast cancer cells. *Nature* **528**, 413-417, doi:10.1038/nature16140 (2015).

25 Liu, Y. *et al.* Tumor Exosomal RNAs Promote Lung Pre-metastatic Niche Formation by Activating Alveolar Epithelial TLR3 to Recruit Neutrophils. *Cancer cell* **30**, 243-256, doi:10.1016/j.ccell.2016.06.021 (2016).

26 Wang, T. T. *et al.* Tumour-activated neutrophils in gastric cancer foster immune suppression and disease progression through GM-CSF-PD-L1 pathway. *Gut* **66**, 1900-1911, doi:10.1136/gutjnl-2016-313075 (2017).

27 Giese, M. A., Hind, L. E. & Huttenlocher, A. Neutrophil plasticity in the tumor microenvironment. *Blood* **133**, 2159-2167, doi:10.1182/blood-2018-11-844548 (2019).

28 Qin, H. *et al.* Targeting tumor-associated myeloid cells for cancer immunotherapy. *Oncoimmunology* **4**, e983961, doi:10.4161/2162402X.2014.983761 (2015).

29 Zhang, P. *et al.* Therapeutic targeting of tumor-associated myeloid cells synergizes with radiation therapy for glioblastoma. *Proceedings of the National Academy of Sciences of the United States of America* **116**, 23714-23723, doi:10.1073/pnas.1906346116 (2019).

30 Van Coillie, S., Wiernicki, B. & Xu, J. Molecular and Cellular Functions of CTLA-4. *Advances in experimental medicine and biology* **1248**, 7-32, doi:10.1007/978-981-15-3266-5_2 (2020).

31 Eri, R., Kodumudi, K. N., Summerlin, D. J. & Srinivasan, M. Suppression of colon inflammation by CD80 blockade: evaluation in two murine models of inflammatory bowel disease. *Inflammatory bowel diseases* **14**, 458-470, doi:10.1002/ibd.20344 (2008).

32 Agraz-Cibrian, J. M. *et al.* Impaired neutrophil extracellular traps and inflammatory responses in the peritoneal fluid of patients with liver cirrhosis. *Scandinavian journal of immunology* **88**, e12714, doi:10.1111/sji.12714 (2018).

33 Seidel, J. A., Otsuka, A. & Kabashima, K. Anti-PD-1 and Anti-CTLA-4 Therapies in Cancer: Mechanisms of Action, Efficacy, and Limitations. *Frontiers in oncology* **8**, 86, doi:10.3389/fonc.2018.00086 (2018).

34 Zhang, Y., Lee, C., Geng, S. & Li, L. Enhanced tumor immune surveillance through neutrophil reprogramming due to Tollip deficiency. *JCI insight* **4**, doi:10.1172/jci.insight.122939 (2019).

35 Anfray, C., Ummarino, A., Andon, F. T. & Allavena, P. Current Strategies to Target Tumor-Associated-Macrophages to Improve Anti-Tumor Immune Responses. *Cells* **9**, doi:10.3390/cells9010046 (2019).

36 Jiang, T. *et al.* Clinical value of neutrophil-to-lymphocyte ratio in patients with non-small-cell lung cancer treated with PD-1/PD-L1 inhibitors. *Lung cancer* **130**, 76-83, doi:10.1016/j.lungcan.2019.02.009 (2019).

37 Shaul, M. E. & Fridlender, Z. G. Tumour-associated neutrophils in patients with cancer. *Nature reviews. Clinical oncology* **16**, 601-620, doi:10.1038/s41571-019-0222-4 (2019).

38 Fan, X. *et al.* Inflammatory Markers Predict Survival in Patients With Advanced Gastric and Colorectal Cancers Receiving Anti-PD-1 Therapy. *Frontiers in cell and developmental biology* **9**, 638312, doi:10.3389/fcell.2021.638312 (2021).

39 Corti, F. *et al.* The Pan-Immune-Inflammation Value in microsatellite instability-high metastatic colorectal cancer patients treated with immune checkpoint inhibitors. *European journal of cancer* **150**, 155-167, doi:10.1016/j.ejca.2021.03.043 (2021).

40 Capone, M. *et al.* Baseline neutrophil-to-lymphocyte ratio (NLR) and derived NLR could predict overall survival in patients with advanced melanoma treated with nivolumab. *Journal for immunotherapy of cancer* **6**, 74, doi:10.1186/s40425-018-0383-1 (2018).

41 Liu, G. C. *et al.* The Heterogeneity Between Lynch-Associated and Sporadic MMR Deficiency in Colorectal Cancers. *Journal of the National Cancer Institute* **110**, 975-984, doi:10.1093/jnci/djy004 (2018).

42 Liu, C. *et al.* A portable and cost-effective microfluidic system for massively parallel single-cell transcriptome profiling. *bioRxiv*, 818450, doi:10.1101/818450 (2019).

43 Dobin, A. *et al.* STAR: ultrafast universal RNA-seq aligner. *Bioinformatics* **29**, 15-21, doi:10.1093/bioinformatics/bts635 (2013).

44 Butler, A., Hoffman, P., Smibert, P., Papalexi, E. & Satija, R. Integrating single-cell transcriptomic data across different conditions, technologies, and species. *Nature Biotechnology* **36**, 411-420, doi:10.1038/nbt.4096 (2018).

45 Patel, A. P. *et al.* Single-cell RNA-seq highlights intratumoral heterogeneity in primary glioblastoma. *Science* **344**, 1396-1401, doi:10.1126/science.1254257 (2014).

46 Vento-Tormo, R. *et al.* Single-cell reconstruction of the early maternal–fetal interface in humans. *Nature***563**, 347-353, doi:10.1038/s41586-018-0698-6 (2018).

Tables

Table 1. Baseline characteristics of 73 MSI-H CRC patients receiving ICIs

	With inflammatory conditions	Without inflammatory conditions	*P* value
Total	16	57	
Gender			0.533
Male	10 (62.5%)	42 (73.7%)	
Female	6 (37.5%)	15 (26.3%)	
Median age (range)	42 (16-73)	42 (24-71)	0.714
MSI status			0.417
MSI-H	11 (68.8%)	40 (70.2%)	
MSI-L/MSS	4 (25.0%)	8 (14.0%)	
Undetermined dMMR	1 (6.2%)	9 (15.8%)	
Category			0.367
Sporadic	3 (18.8%)	17 (29.8%)	
Lynch-associated	7 (43.7%)	28 (49.1%)	
undetermined	6 (37.5%)	12 (21.1%)	
Histology			0.231
Adenocarcinoma	11 (68.8%)	47 (82.5%)	
Mucinous Adenocarcinoma	5 (31.2%)	10 (17.5%)	
ICI monotherapy			0.704
Yes	7 (43.7%)	28 (49.1%)	
No	9 (56.3%)	29 (50.9%)	
First-line chemotherapy prior to ICIs			0.028
Yes	4 (25.0%)	32 (56.1%)	
No	12 (75.0%)	25 (43.9%)	

Table 2. Univariate and multivariate Cox proportional hazards regression for PFS.

Variable	No. of cases	*HR* (95% *CI*)	*P*
MSI status			
MSI-H	52	1.000 (ref)	——
MSI-L/MSS	11	3.536 (1.281~9.759)	0.015
Inflammatory conditions			
No	57	1.000 (ref)	——
Yes	16	5.393 (2.121~13.712)	<0.001
Histology			
Adenocarcinoma	58	1.000 (ref)	——
Mucous adenocarcinoma	15	2.239 (0.867~5.781)	0.096
Multivariable			
MSI status			
MSI-H		1.000 (ref)	——
MSI-L/MSS		2.497 (0.806~7.730)	0.113
Inflammatory conditions			
No		1.000 (ref)	——
Yes		3.637 (1.255~10.538)	**0.017**
Histology			
Adenocarcinoma		1.000 (ref)	——
Mucous adenocarcinoma		1.112 (0.353~3.502)	0.856

Figures

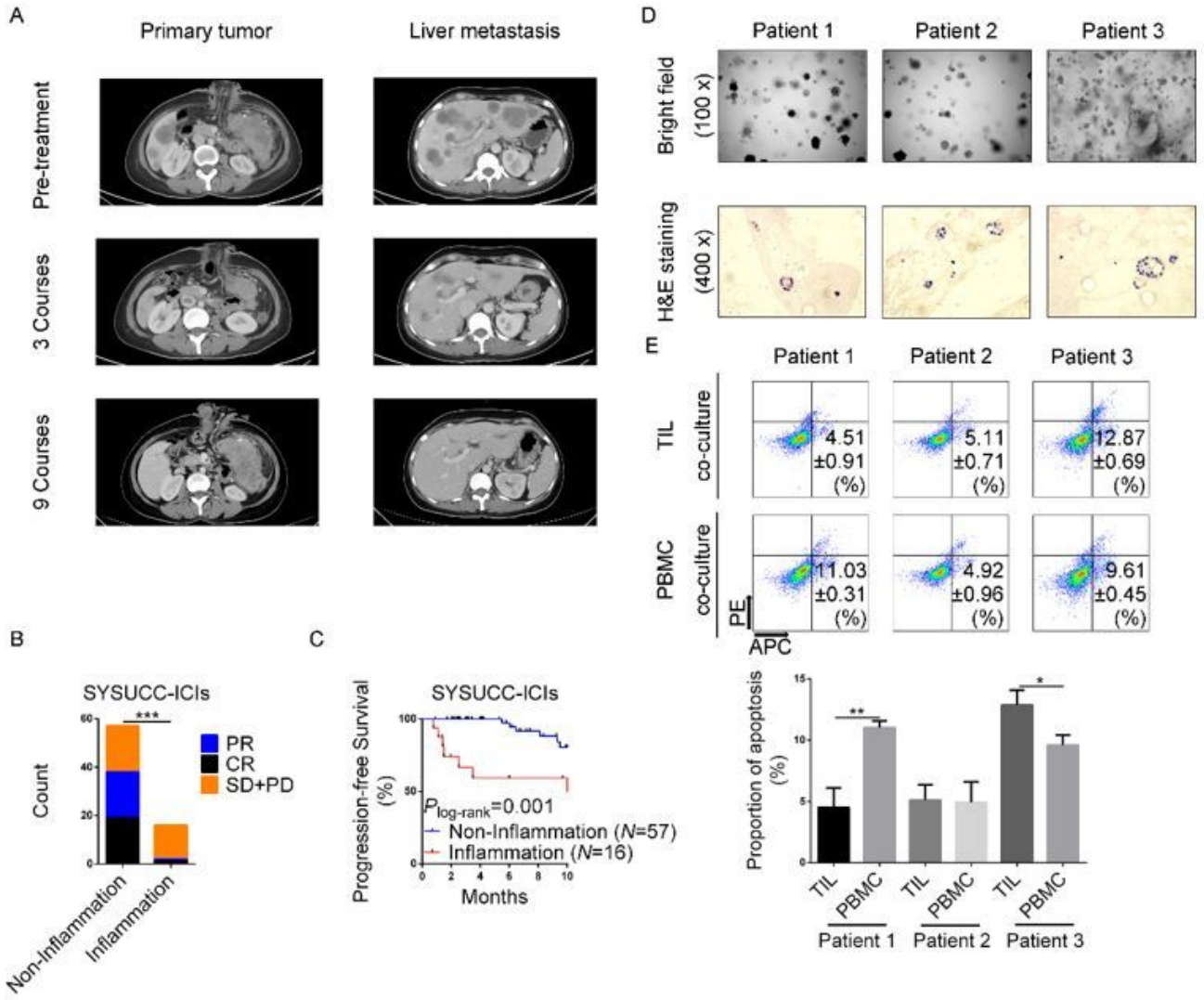

Figure 1

Inflammatory conditions are associated with poor response to ICIs in dMMR/MSI-H CRCs. (A) CT scans were conducted on Patient 1 after 0 courses, 3 courses and 9 courses of Pembrolizumab. Images of the primary tumor and metastatic lesions are shown. (B-C) Tumor response (B) and progression-free survival (C) after ICIs were compared between dMMR/MSI-H CRC patients with and without inflammatory conditions. (D) Bright field (100x) and H&E staining (400x) of tumor organoids from Patient 1, Patient 2 and Patient 3 are shown. (E) Tumor organoids were cocultured with paired TILs or PBMC-derived T cells for 6 hours and were then separated for apoptosis assays. PR: partial response; CR: complete response; SD: stable disease; PD: progressed disease; *: 0.01≤P≤0.05; **: 0.001≤P≤0.01; ***: 0.0001≤P≤0.001.

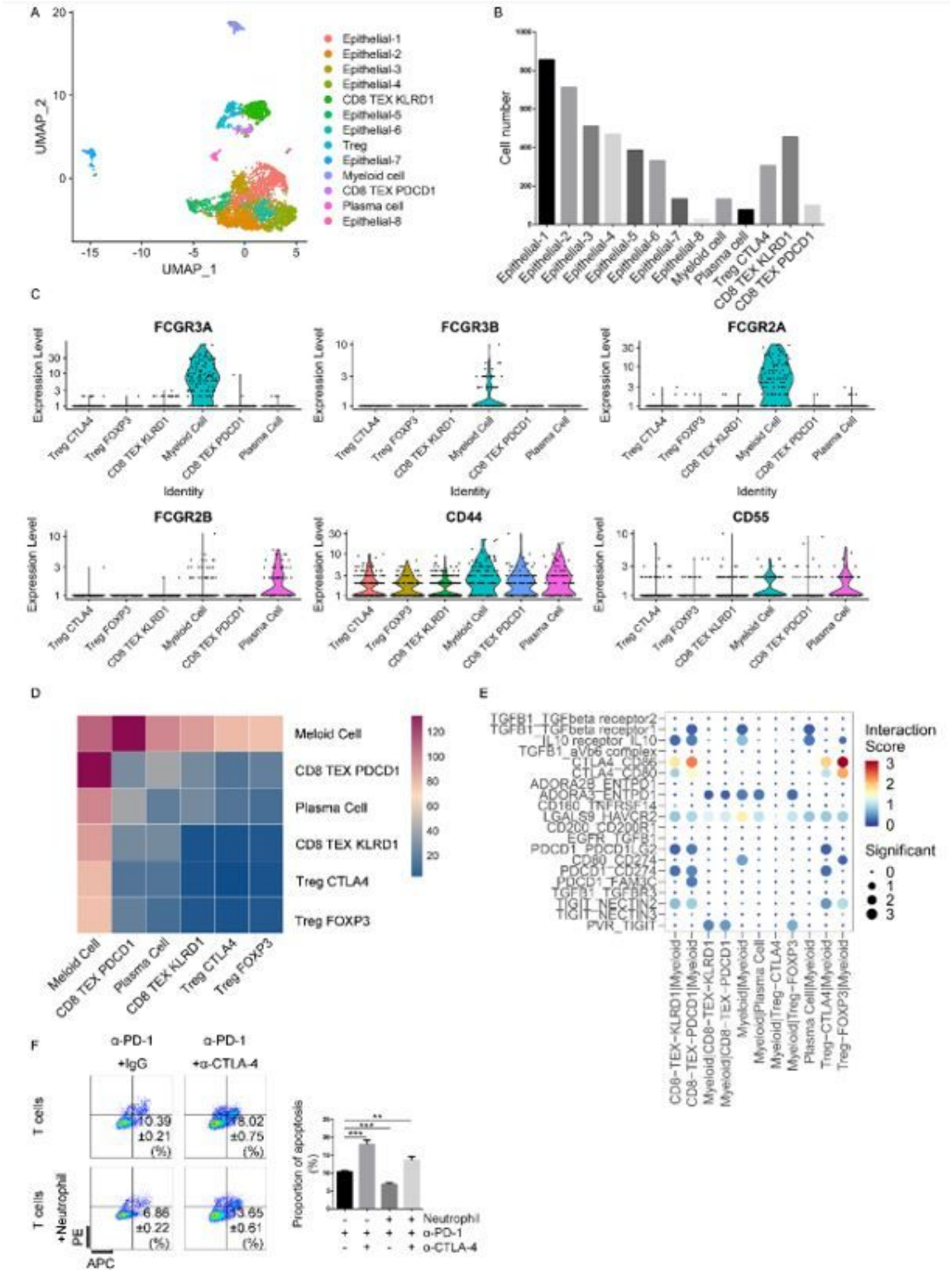

Figure 2

Single-cell sequencing reveals an inhibitory role of neutrophils in tumor immune status. (A-B) The 4489 qualified cells were divided into eight epithelial cells and five groups of immune cells using a UMAP plot (A). Cell number in each cluster is shown (B). (C) The expression level of neutrophil marker genes in each cluster is shown using a violin plot. (D-E) Interactions between subtypes of immune cells were analyzed. Functional phenotypes and predicted interactions of myeloid cells and T cells (D) and ligand-receptor

interactions in immune checkpoints between immune cells are shown (E). (F) Murine T cells prestimulated with or without neutrophils in the presence or absence of CTLA-4 neutralizing antibodies (α-CTLA-4) were pretreated with PD-1 neutralizing antibodies (α-PD-1) and then cocultured with CT26 cells for 12 hours. Apoptosis assays were used to evaluate the proportion of apoptosis in each group. **: 0.001≤P≤0.01; ***: 0.0001≤P≤0.001.

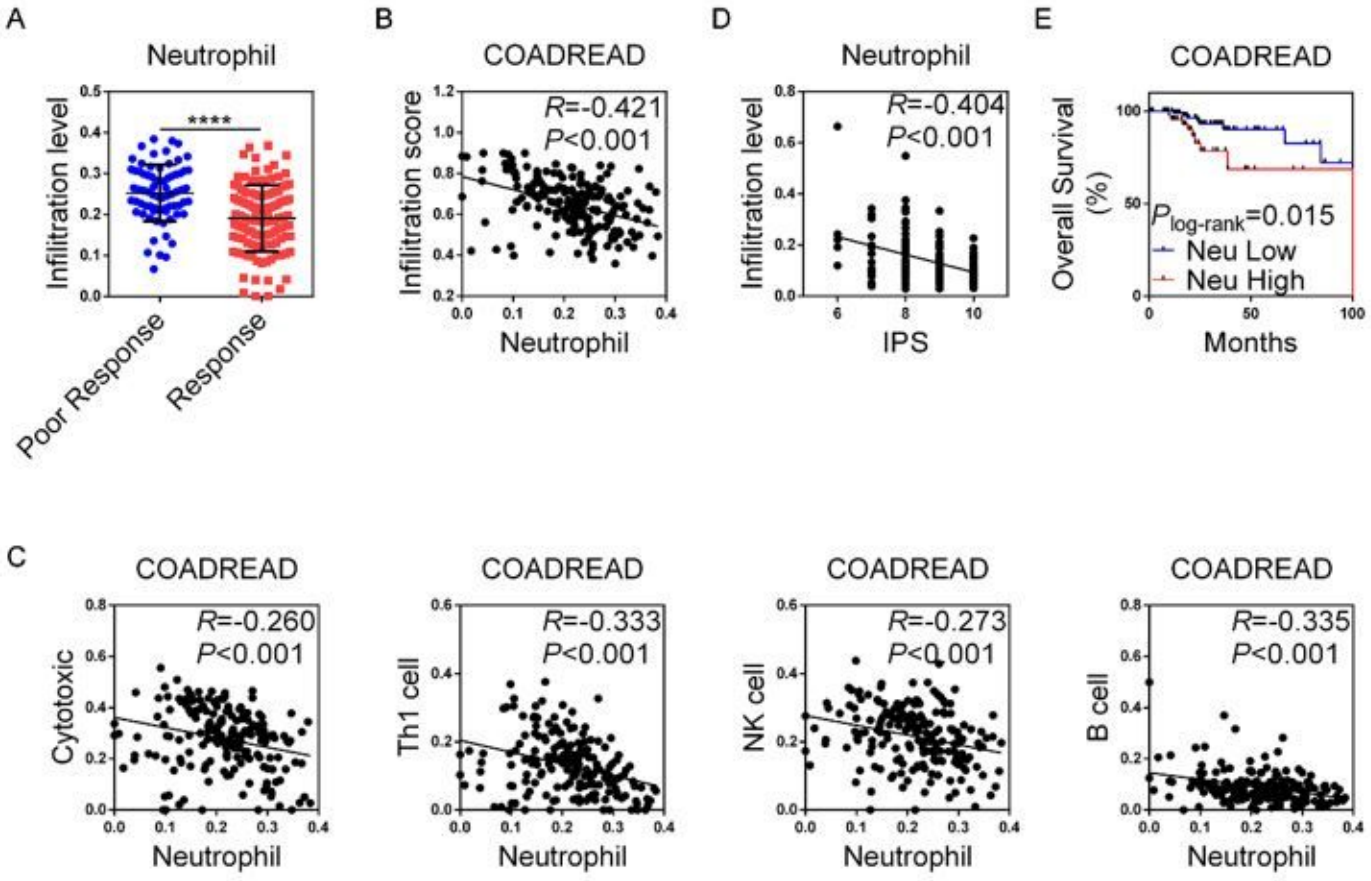

Figure 3

Elevated neutrophil infiltration is associated with poor immune status and poor response to ICIs in the TCGA. (A) Data of MSI CRC cases in the TCGA were analyzed using ImmunCellAI. Infiltration levels of neutrophils were compared between patients who predicted poor response and good response to ICIs. (B) Correlation between total infiltration scores and neutrophil infiltration levels was analyzed. (C) Correlations between the infiltration levels of cytotoxic T cells, Th1 cells, NK cells, B cells and neutrophils were analyzed. (D-E) Data of MSI CRC cases in the TCGA were analyzed using TIMER and TCIA. The correlation between neutrophil infiltration level and IPS was analyzed (D), and overall survival was compared between patients with high and low neutrophil infiltration levels (E). Neu: neutrophils; ****: P≤0.0001.

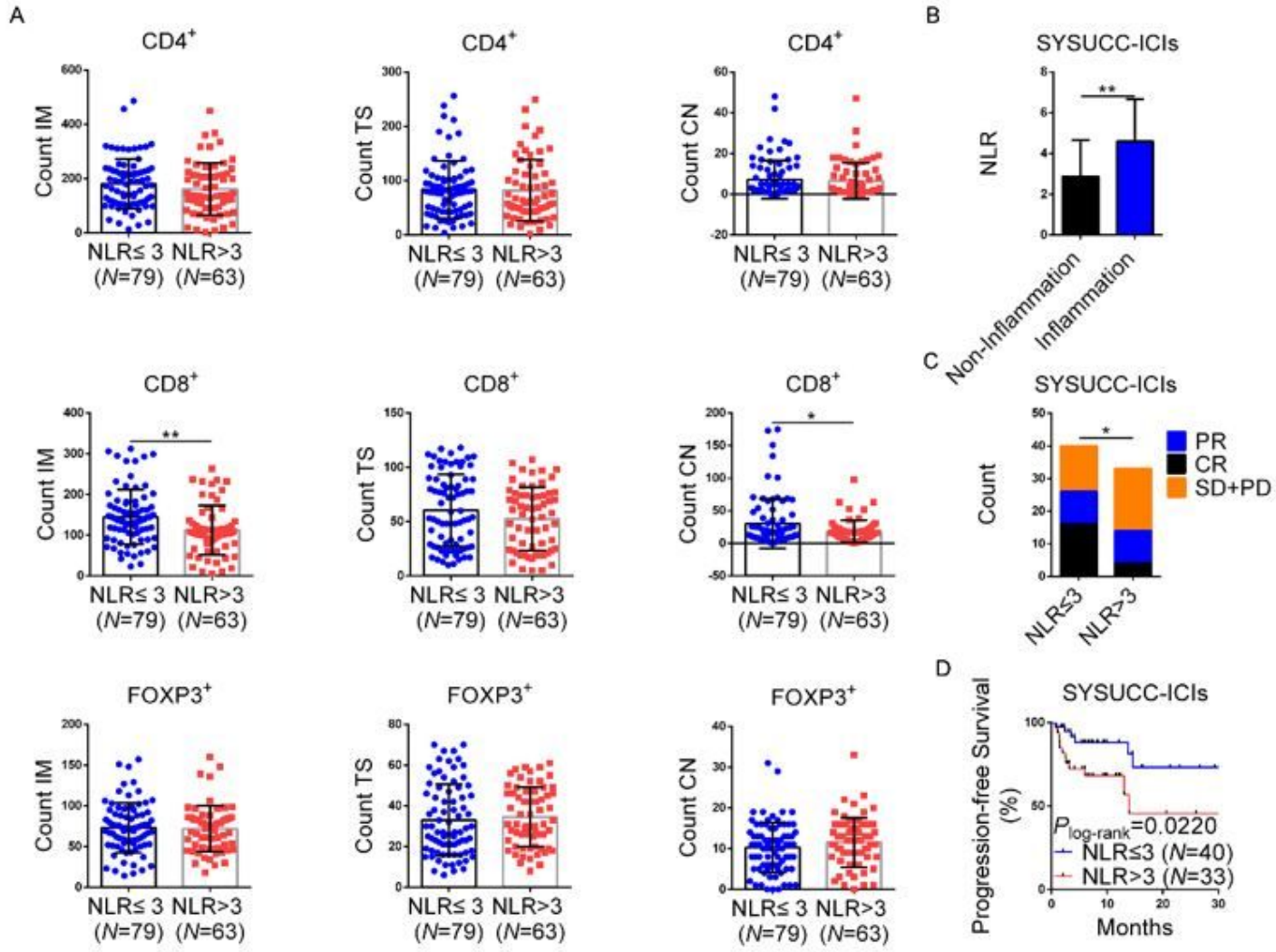

Figure 4

Elevated NLR is associated with poor immune status and resistance to ICIs. (A) In a cohort of 142 surgically resected dMMR CRCs, the CD4+, CD8+ and FOXP3+ TILs in the IM, TS and CN were compared between patients with NLR≤3 and NLR>3. (B) In 73 dMMR/MSI-H CRCs receiving ICIs, NLR was compared between patients with and without inflammatory conditions. (C-D) Short-term response (C) and PFS (D) after ICIs were compared between dMMR/MSI-H CRC patients with NLR≤3 and NLR>3. *: 0.01≤P□0.05; **: 0.001≤P□0.01.

Supplementary Files

This is a list of supplementary files associated with this preprint. Click to download.

- Supplementaryfigures.docx